IIETA International Information and Engineering Technology Association
Advancing the World of Information and Engineering

Blood Pressure Estimation from Photoplethysmogram Using Hybrid Bidirectional Long Short-Term Memory and Convolutional Neural Network Architecture

Ahmed Ezzat[1,2], Osama A. Omer[1*], Usama S. Mohamed[3,4], Ahmed S. Mubarak[1]

[1] Faculty of Engineering, Aswan University, Aswan 81542, Egypt
[2] Department of Electronics and Communications, Luxor Higher Institute of Engineering and Technology, Luxor 85834, Egypt
[3] Department of Electrical Engineering, Faculty of Engineering, Assiut University, Assiut 71518, Egypt
[4] Faculty of Engineering, Sphinx University, Assiut 71515, Egypt

Corresponding Author Email: omer.osama@aswu.edu.eg

ABSTRACT

Cardiovascular diseases are a leading cause of death worldwide. Invasive blood pressure monitoring is often considered the most reliable method, but it requires surgery and can lead to multiple complications. Consequently, there is a need for a non-invasive technique to predict the continuous arterial blood pressure (ABP) waveform using photoplethysmography (PPG) signals. Predicted ABP can provide more comprehensive information than isolated blood pressure values. To this end, we propose a deep learning-based approach for predicting continuous ABP beats from PPG input beats. Furthermore, an in-depth study is presented, exploring different 1-D and 2-D deep learning networks for estimating ABP beats from PPG beats across various transformation feature domains. We introduce a scattering wavelet transform as a novel transformation domain for ABP estimation, combined with a hybrid bidirectional LSTM and CNN neural network architecture (conv-BiLSTM). The performance of the proposed method is compared with different deep neural networks (DNNs). Specifically, we pit it against two 1-D DNNs (LSTM and BiLSTM), a 1-D audio network (crepe), and two 2-D image DNNs (Alexnet and VGG19) in terms of mean absolute error (MAE) and standard deviation (STD). Simulation results demonstrate that our proposed conv-BiLSTM with scattering transformation achieves the lowest STD and MAE for estimating diastolic blood pressure (DBP). However, for systolic blood pressure (SBP) estimation, the proposed conv-BiLSTM neural network attains the minimum STD and MAE when employing the discrete cosine transform.

1. INTRODUCTION

The World Health Organization (WHO) has reported that globally, cardiovascular diseases (CVDs) account for approximately 17.7 million deaths. By 2030, this figure is projected to escalate to nearly 23 million annually. Therefore, the frequent monitoring of blood pressure is crucial, and if found to be elevated, interventions such as medications need to be employed to manage optimal blood pressure levels [1].

Hypertension, colloquially known as high blood pressure, is a condition where an individual's blood vessels narrow due to the accumulation of fats and free agents, leading to a persistent rise in blood pressure. Consequently, the measurement and control of blood pressure during medical procedures and outpatient visits are critical in the assessment of hypertension. The most reliable and prevalent tool for measuring blood pressure is auscultation with a mercury or electronic sphygmomanometer. Physicians use Korotkoff sounds to determine systolic and diastolic blood pressure [2].

While this blood pressure measurement method is straightforward and provides adequate values for analysis, it carries certain drawbacks. For instance, the discomfort associated with increased cuff pressure can induce stress in the patient, leading to inaccurate blood pressure measurements [3]. Moreover, this method fails to provide continuous beat-to-beat measurements needed to evaluate high-frequency blood pressure changes, as the inflation, deflation, and normalization process can span several seconds. Hence, there has been a longstanding pursuit in the research community to devise methods for continuous, cuff-free, and non-invasive blood pressure monitoring using biomedical data.

Photoplethysmography (PPG) waveforms offer a less intrusive and accurate approach to hypertension monitoring. The fundamental principle of PPG is simple: it involves the illumination of skin and subsequent measurement of its light absorption. Consequently, a typical PPG sensor comprises an LED light source and a photodetector [4].

Photoplethysmography is employed in various ways to estimate blood pressure. This study anticipates the continuous arterial blood pressure signal shape from the PPG signal. To date, no research has directly predicted arterial blood pressure waveforms from PPG signals using one-dimensional and two-dimensional deep learning networks with different transformation features, despite numerous efforts to

investigate PPG-arterial blood pressure signals. Our work focuses on the beat-by-beat analysis of PPG-arterial blood pressure correlation.

The primary contributions of this paper can be summarized as follows:

1. Comparative study of different one-dimensional and two-dimensional deep learning networks for estimating arterial blood pressure based on the PPG signal.
2. Comparative study of the impact of the feature domain on arterial blood pressure estimation and blood pressure estimation using different deep neural networks.
3. Comparative study of different optimization algorithms for different transformation feature domains in deep neural networks for estimating arterial blood pressure from photoplethysmography.
4. Proposal of a scattering wavelet transform with convolutional bidirectional long short-term memory deep neural network as a promising feature domain for arterial blood pressure and blood pressure estimation.

2. RELATED WORK

Deep learning algorithms, trained on biological signals, have been increasingly utilized in blood pressure waveform estimation due to their ability to automatically learn essential features. Numerous methods for predicting blood pressure from photoplethysmogram signals have been published, though fewer techniques focus specifically on arterial blood pressure waveform prediction from photoplethysmogram data.

Biological signals such as electrocardiograms (ECGs) and photoplethysmograms (PPGs) form the basis for much of the published work on blood pressure waveform prediction.

The related work for estimating blood pressure or arterial blood pressure signals can be broadly classified into three categories: traditional methods for blood pressure estimation, deep learning-based blood pressure estimation, and arterial blood pressure waveform estimation.

2.1 Traditional methods for BP estimation

When examining traditional methods for blood pressure estimation, we can categorize them into two groups: those that utilize the photoplethysmogram (PPG) signal and those that do not.

Pulse Transit Time (PTT): One approach to measuring blood pressure without a cuff is the Pulse Transit Time (PTT) method. PTT refers to the duration required for a pressure wave to travel between two arterial sites [5]. The relationship between blood pressure and PTT under various conditions was explored in the study [6].

Pulse Arrival Time (PAT): Pulse Arrival Time is the time interval between the electrical stimulation of the heart and the arrival of the pulse wave at a specific location on the body. The Pre-ejection Period (PEP) delay, which includes the Pulse Transit Time, isovolumic contraction duration, and ventricular electromechanical delay, contributes to PAT [5]. Despite its limited accuracy in diastolic pressure measurement, PAT continues to be used [7].

Pulse Wave Velocity (PWV): Pulse Wave Velocity is another method that can be utilized for blood pressure estimation without a cuff, and it has demonstrated good performance [8].

Pulse Wave Analysis (PWA): Pulse Wave Analysis refers to the process of signal processing and feature extraction from the PPG waveform to identify distinctive characteristics. Multiple studies [9] have explored the potential of a single PPG sensor for making cuff-free, continuous blood pressure predictions.

2.2 PPG-based BP estimation

On the other hand, machine learning (ML) algorithms are suitable due to their strong ability to learn complex mapping relationships between inputs and outputs.

Linear Regression (LR): Teng and Zhang conducted an initial study on estimating blood pressure using PPG signals [10]. Given the high correlation between diastolic blood pressure (DBP) and systolic blood pressure (SBP) [11], learning both targets within a single model structure could enhance estimation by learning common data representations. The Taguchi signal-to-noise ratio method for monitoring systolic blood pressure was proposed in the research [12], while a PLS-based SBP estimation was introduced in 2019 [13].

Regression Tree (RT): In the research [14], the predictive efficacy of three machine learning techniques — the Multilayer Perceptron (MLR), Support Vector Machine (SVM), and Regression Tree (RT) — was examined for SBP and DBP prediction. Their research [15] suggested that Heart Rate (HR) and Pulse Transit Time (PTT) were the most significant indicators of cardiovascular health.

KNN-based Methods: the research [16] proposed a continuous, high-precision arterial blood pressure estimation method using machine learning algorithms and the PPG signal. Nine morphological features were derived from PPG period signals. Machine learning techniques included LR, KNN, LASSO, CART, and Elastic Net, with KNN performing best in algorithm utility tests.

Decision Tree (DT): Using the MIMIC II dataset, the research [17] extracted features from unsuitable whole-based models of PPG signals. Decision Tree, SVM, Adaptive Boosting Regression, and Random Forest were used to predict blood pressure. This continuous, non-invasive method requires no calibration. The study met the AAMI standards for DBP and Mean Arterial Pressure (MAP) but not for SBP.

Support Vector Machine (SVM): Data mining and a mechanism-driven model were used to estimate blood pressure in the research [18]. SVM outperformed MLR, endorsing the nonlinear relationship between features and blood pressure. Researchers measured DBP and SBP from a PPG signal and extracted 14 features, including PTT, pulse pattern, and heart rate [19]. Support Vector Regression (SVR) was used to determine blood pressure across all methods.

2.3 Deep learning-based BP estimation

Recurrent Neural Network (RNN): In the research [10], an Artificial Neural Network-Long Short-Term Memory (ANN-LSTM) model was used to develop a waveform-based approach for continuously estimating blood pressure using Electrocardiogram (ECG) and Photoplethysmogram (PPG) waveforms. Artificial intelligence has aided in utilizing cutaneous photoplethysmography for blood pressure measurement during cardiac resuscitation. It was confirmed

through studies that an LSTM model with a single PPG could predict blood pressure [20]. Time-frequency-chaotic features were identified from ECG and PPG data. The performance was compared against Linear Regression (LR), tagged tree, coarse tree, Gaussian Process Regression (GPR), Gaussian Support Vector (GSV), and dynamic learning models like Nonlinear AutoRegressive Exogenous model-Neural Network (NARX-NN), RNN, and LSTM [21].

Convolutional Neural Network (CNN): Two phases were involved in the proposed model of the research [22]. The initial phase utilized two CNNs to extract characteristics from PPG segments prior to predicting Systolic Blood Pressure (SBP) or Diastolic Blood Pressure (DBP). Following this, Long Short-Term Memory (LSTM) was used to maintain temporal dependencies. Incorporating the separation component, the research [23] proposed a fully convolutional network for time and frequency domain inputs. Furthermore, the research [24] demonstrated a complex deep network for physiology or medicine using derivative products of PPG and frequency domain PPG information.

2.4 ABP waveform estimation

In the research [25], the Nonlinear AutoRegressive eXogenous model (NARX) was implemented as an Artificial Neural Network (ANN) model applied to Photoplethysmogram (PPG), Electrocardiogram (ECG), or both. In the research [26], two deep learning models were used to generate blood pressure waveform estimates. An approximation network, a one-dimensional U-Net network, was used to estimate the pattern using a PPG signal. The expected blood pressure waveforms were then refined using an iterative network. The model was further enhanced using a 1D Multi Res U-Net model. According to another study [27], a 1D adapted U-Net network can be used to evaluate blood pressure waveforms.

3. THE PROPOSED ABP ESTIMATION BASED ON DEEP LEARNING

Due to the structural similarity, all systems in this paper used PPG beats to estimate ABP beats. The procedure for estimating ABP beats with deep learning is depicted in Figure 1 using PPG beats. The proposed systems are established in several stages: (1) dataset setup, (2) data prepossessing, (3) Different Feature domains, (4) data partitioning, (5) Different Deep Learning NNs training models, (6) ABP Model Estimation. The following sub-sections will implement detailed discussion for each stage.
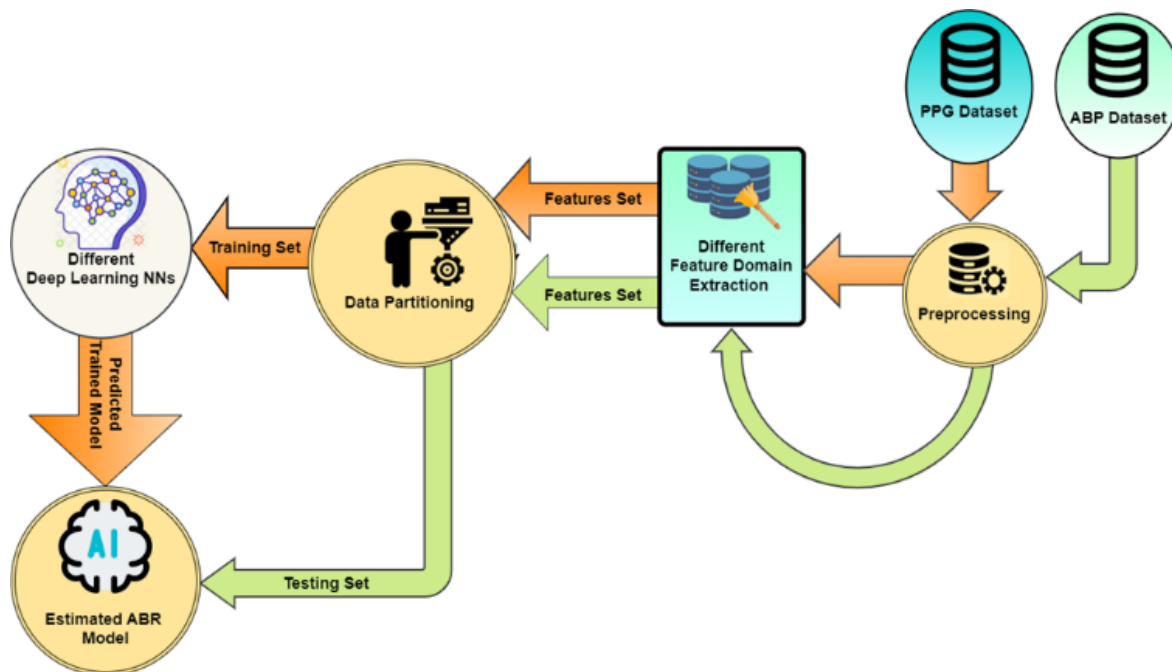

Figure 1. Block diagram for the proposed system model

3.1 Dataset setup

Physionet MIMIC II (Multi-parameter Intelligent Monitoring in Intensive Care) contains the joint PPG-ABP data used to teach deep learning models [28]. The research [29] arranged the dataset. It has nearly 12,000 subject. Each record includes 125 samples per second ECG (channel II), PPG (fingertip), and ABP (invasive arterial blood pressure, mmHg). We are particularly interested in PPG and marked ABP signals. To filter and handle records, 1024 sample parts are used. For good results, the research [30] prepare a dataset without artefacts to train and test a deep learning estimator for a combined PPG-ABP cleaning method. We use 175000 cleared beats instead of 309000 uncleaned beats because

uncleaned data can fool deep networks. The dataset is available at their website (https://cibpm.com/).

3.2 Data prepossessing

If the PPG signal's morphology doesn't change, just PPG signals can be pre-processed using enhancing techniques like bandpass filtering in the frequency range [0.5-8] Hz. When trying to increase the quality of the ABP signal, the magnitude of the signal changes, which in turn changes the BP value, rendering the improvement impossible. ABP signals or beats that are heavily distorted must be excluded [30]. The resulting pre-processed signals were used to extract features and train the learning models.

3.3 Transformation features domain

A comparison is presented in this section between different transformation feature domains and combinations between them (Time domain (TD), Discrete cosine transform (DCT), Discrete Wavelet transform (DWT) and Scattering Wavelet transform (SWT)).

3.3.1 Time domain (TD)

In this Proposed system, the time domain is the original signal for the PPG and ABP signal without any transformation techniques.

3.3.2 Discrete cosines transform (DCT)

The discrete cosine transform is an orthogonal transformation of a real series. Discrete cosine transforms (DCTs) are used to decompose signals into their fundamental frequency components [31].

In this article, the discrete cosine transform (DCT) is applied to PPG signals to determine their characteristics. After the DCT transformation, we find that the initial points of the DCT transform sequence contain the majority of the PPG signal's energy. So, the PPG signal's initial points after DCT are used as the feature to learn to predict ABP.

3.3.3 Discrete wavelet transform (DWT)

Physiological signals like PPG, ECG, and ABP signals have been illustrated and analysed using wavelets because of their compact support. The ABP waveform contains clinically significant information on multiple time scales. As a result, the wavelet method is suitable because it can focus on varying sizes of signals, much like a mathematical microscope [32].

3.3.4 Scattering wavelet transform (SWT)

The suggested approach estimates the ABP signal from the PPG signal using a signal processing technique called wavelet scattering transform [33]. Jean Effil and Rajeswari [34] accurately estimated BP from PPG signals using a WST and LSTM algorithm. The WST is divided into three stages that cascade:

First, the signal x is decomposed and convolved at center frequency λ with a dilated mother wavelet ψ yielding $x*\psi_\lambda$.

Second, when a nonlinear modulus operator is applied to a convolved signal, the frequency of the signal increases, which may make up for the data lost during down sampling.

Third, the absolute convolved signal is subjected to a low-pass/time-average filter implemented as a scale factor, yielding $|x*\psi_\lambda|*\varnothing_J$.

3.3.5 Combinations for the model

In this paper used seven input-output combinations using different feature domain. These combinations are tabulated in Table 1 as follow:

Table 1. Combinations between input-output for different feature domains

Scheme	PPG Input Domain	ABP Output Domain	Abbreviation
TT	TD	TD	PPG-TD/ABP-TD
CT	DCT	TD	PPG-DCT/ABP-TD
CC	DCT	DCT	PPG-DCT/ABP-DCT
WT	DWT	TD	PPG-DWT/ABP-TD
WW	DWT	DWT	PPG-DWT/ABP-DWT
ST	SWT	TD	PPG-SWT/ABP-TD
SW	SWT	DWT	PPG-SWT/ABP-DWT

3.4 Transfer learning

3.4.1 1-D NN

LSTM: RNNs fix the common neural network's linear data issues. RNN efficiency decreases with sequence length. LSTMs are intended to solve this problem [35].

A CNN or RNN is a self-learning neural network. LSTM, the most common RNN, mitigates the fading scaling issue. An input gate sends activation into a memory block, and an output gate sends it out and into the network. A forget gate was integrated into the memory block to sense the subsequent cell's internal state and provide an input to the cell via self-repetitive communication to forget or reset the cell's memory [36].

Lee et al. [37] trained a Bidirectional LSTM network to estimate BP across heartbeats using data from a Ballistocardiogram (BCG), PPG, and ECG.

BiLSTM: Because LSTM is unidirectional and cannot detect relationships with previous words, BiLSTM is used in practice. Bi-LSTM [38] is made up of two LSTM modules facing each other, one front-to-back and one back-to-front. The learnable parameters of two LSTMs with the identical inputs can be substantially different. The Bi-LSTM output is formed by concatenating the outputs of two LSTMs. By using two independent hidden layers that forward to the same output layer, bidirectional RNNs (BRNNs) [39] are able to process data in both directions.

ConvBiLSTM: CNN is a cutting-edge method for automatic feature extraction, and LSTM is an efficient time series data analysis method that can manage long sequential data. They proposed a two-hierarchical model with a one-dimensional CNN and Bi-LSTM for featureless-based BP prediction in the research [40]. The lower hierarchy extracts feature automatically, while the upper learns their temporal connection. The lower hierarchy extracts traits automatically, and the upper learns their temporal relationship. CNN layers receive resampled PPG segments. From CNN layer output, BiLSTM layers produce SBP and DBP regression results.

Using a CNN-BiLSTM, the research [41] recreates central artery pressure from radial arterial pressure patterns. The CNN-BiLSTM model for reconstructing central artery pressure was tested in 62 patients by invasively measuring central aortic and radial arterial pressure patterns before and after therapy.

Crepe: The CREPE model [42] is a time-domain CNN. Fully supervised training minimises entropy loss between ground truth pitch notes and model output.

We know no one estimates BP using the CREPE network. This paper proposed this network for estimating ABP from PPG signal.

3.4.2 2-D NN

AlexNet: AlexNet, ResNet, and the MIMIC dataset model were examined in the research [43]. Transfer learning was used to adjust the final layer of models pre-trained with rPPG data. This study studied how titration affected blood pressure estimate.

Some works have used a pre-tested ImageNet model to convert one-dimensional physiological potential (PPG) data into two-dimensional images [44]. The Visibility Graph (VG) method creates images from PPG data. (which are only one dimension). This innovative method kept the temporal frequency information in the PPG signals and allowed transform learning by using previously validated CNN models on the extensive ImageNet database.

VGG-19: DNNs were used to predict SBP and DBP in this study [45]. Other researchers offered two independent pathways and multistage models for direction-specific parameter extraction and estimation. Considering SBP-DBP correlation, this method enhanced model sensitivity.

Wang et al. [44] proposed a VGG19 neural network to turn one-dimensional PPG signals into images using Visibility Graph (VG) method. allowed using BP-trained image classifiers.

3.5 Study of optimization techniques

Training a DNN can take a significant amount of time and computing power, therefore finding an efficient optimization strategy is of great interest. We use in this paper the most three popular algorithms. Adaptive Momentum optimizer (ADAM), Stochastic Gradient Descent with Moment (SGDM), and Root Mean Square Propagation (RMSProp).

3.6 The proposed method

The suggested system is based on the signals from photoplethysmography and employs deep learning models to determine the ABP signals on a per-beat basis. Specifically, the suggested system is divided into two distinct phases: the scattering wavelet transforms phase and the Conv-BiLSTM DNN phase.

First, the scattering transform produces a useful, stable, and signal-invariant representation of signal features. Wavelet decomposition, modular operation, and LPF achieve this. Iteratively calculate the input signal and wavelet modulus function. The wavelet modulus operator's constant part S_x is used for coefficient output. The next-order transformation's covariant input is U_x. Reconstruct high-frequency data lost while the invariant component was operating.

All of the orders 0th through m-th of the scattering transform's output sets make up the final scattering coefficients:
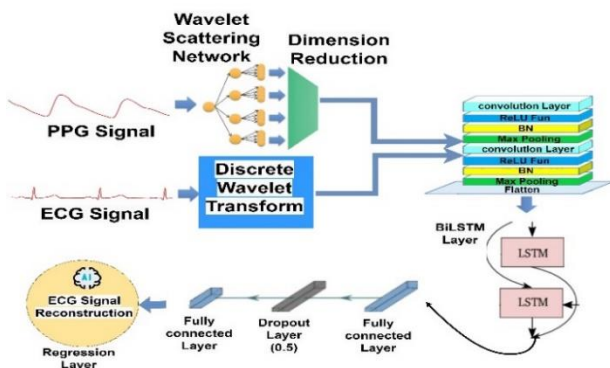
$$Sx = \{S_0 x, S_1 x, \dots, S_m x\} \tag{1}$$

Figure 2. Block diagram for the proposed scattering wavelet transform with conv-BiLSTM DNN for ABP and BP estimation

The scattering transform structure diagram is shown in the first stage of Figure 2.

The proposed network is two-tiered. CNN layers extract lower-hierarchy useful information. BiLSTM estimates at the highest level by learning temporal links between lower-level traits. A block diagram for the whole proposed system is shown in Figure 2. The proposed system is consisting of three stages. These stages are described in the following steps.

Signal transformation: During this phase, the PPG and ABP signals are examined in their entirety, without undergoing any form of segmentation. The central concept lies in examining both signals in the frequency domain, where it is necessary for both signals to display comparable spectral characteristics. Both the PPG and ABP signals originate from the same pulsating source, namely the heart. The PPG and ABP signals exhibit characteristics of quasi-periodicity, as they possess fundamental frequencies that are identical. Both signals must pass through the transformation domain before entering the learning stage. The study examines four feature domains, namely the time domain, DCT domain, DWT domain, and SWT domain, through the implementation of seven distinct combinations.

Training Phase: The estimation of ABP beats is conducted through the utilization of a Proposed Conv-BiLSTM sequence-to-sequence regression model, where the PPG features are employed as predictors. In this study, we propose a methodology for reconstructing ABP beats from PPG beats, utilizing a combination of CNN and BiLSTM models. The initial approach to enhancing the model's resilience to deformation involves the utilization of CNNs [46]. CNNs have demonstrated their efficacy in the field of image recognition [47] making them a suitable choice for extracting spatial features. After obtaining the spatial features, we proceed to utilize the BiLSTM model to extract temporal features from the output of the CNN. The utilization of BiLSTM, a classifier that incorporates both forward and backward phases, is recommended for the prediction of ABP waveforms. In contrast to conventional RNN and LSTM models, BiLSTM effectively mitigates the problems of gradient vanishing and gradient exploding, while maintaining a high level of accuracy.

Regression: The model's final stage has two fully connected levels separated by a Dropout layer. After this layer the regression layer of the ABP, SBP and DBP are obtained.

Resampled PPG segments feed CNN layers. The CNN layers will feed the BiLSTM layers SBP and DBP regression data. Figure 2 shows the overall case. The model uses a two-layer, one-dimensional convolutional neural network (CNN) with ReLU, BN, and maximum pooling activation functions. (max pooling).

After that, the most recent max-pooling layer output is smoothed for BiLSTM layer input. The model's final layer has two fully connected levels separated by a Dropout layer. This layer generates SBP and DBP regression data.

The context in which blood pressure is estimated involves the estimation of arterial blood pressure (ABP), which can be conceptualized as a representation of blood pressure in continuous time. In this section, the estimation of ABP beats is conducted based on the corresponding PPG beats. This is achieved through the utilization of the convBiLSTM network, which has been proposed for this purpose. The network includes a sequence regressor output layer with dimensions of 120×1. Given that the output is in the form of a sequence, our focus lies on the time series of ABP.

4. SIMULATION RESULTS

Our models were trained with 90% of the data, 10% of the training data used for cross validation and our models tested with 10%. Training and testing samples were distinct and separated. Using the training dataset, the network's parameters are modified based on training error. Thus, network efficiency can be objectively assessed. ADAM, SGDM, and RMSProp optimizers were used to train the model, and the RMSE loss function was chosen. 0.001, 50, and 20 were the initial learning rate, max epochs, and minimal batch size. The network's learning rate and batch size were optimised through testing. All codes were written in MATLAB.

4.1 ABP waveform simulation analysis results

Table 2 presents RMSE values pertaining to the estimated ABP beats. These estimations were obtained using the ADAM optimizer in conjunction with various Deep Neural Networks (DNNs) and distinct feature domains. The ConvBiLSTM neural network, as proposed, demonstrates superior performance compared to the best RMSE achieved by utilizing the combination of scattering wavelet transform (SWT) applied to PPG and discrete wavelet transform (DWT) applied to ABP. The convBiLSTM neural network with SW feature domain demonstrates the lowest RMSE of 6.53, indicating superior performance when optimized using the ADAM optimizer.

Table 3 presents the RMSE values for the estimated ABP beats. These estimates were obtained using the SGDM optimizer, employing various DNNs and distinct feature domains. The ConvBiLSTM neural network, as proposed, demonstrates superior performance compared to the best RMSE achieved using SW. The CT transformations involve the combination of DCT applied to PPG and the time domain of ABP, resulting in improved RMSE for the BiLSTM neural network. The BiLSTM neural network with CT feature domain achieves a RMSE of 6.11 for the PPG2ABP task, making it the optimal choice when using the SGDM optimizer.

Table 4 presents the RMSE values obtained from the estimation of ABP beats using the RMSProp optimizer across various DNNs and feature domains. The ConvBiLSTM neural network, as proposed, exhibits superior performance compared to the best RMSE achieved using SW. The experimental results indicate that convBiLSTM NN with SW feature domain produces the most favorable output when optimized using the RMSProp optimizer. The RMSE achieved by this model for the PPG2ABP task is 6.35.

4.2 ABP waveform reconstruction results

Figure 3 presents an illustrative instance of the reconstructed ABP beats, utilizing distinct feature domains and diverse DNNs, in comparison to the ground truth ABP beat. This comparison is conducted under the ADAM optimizer. The figure demonstrates a strong correlation between the estimated ABP beat obtained through the utilization of SW and ST, and the ground truth ABP beat when using the proposed ConvBiLSTM NN compared to various other DNNs.

(a)

(b)

(c)

(d)

(e)

(f)

Figure 3. ABP signal Reconstruction from different DNN and different Transformation combinations at ADAM optimizer (a) LSTM, (b) BiLSTM, (c) Proposed ConvBiLSTM, (d) Alexnet, (e) VGG19, and (f) crepe

Figure 4. ABP signal Reconstruction from different DNN and different Transformation combinations at SGDM optimizer (a) LSTM, (b) BiLSTM, (c) Proposed ConvBiLSTM, (d) Alexnet, (e) VGG19, and (f) crepe
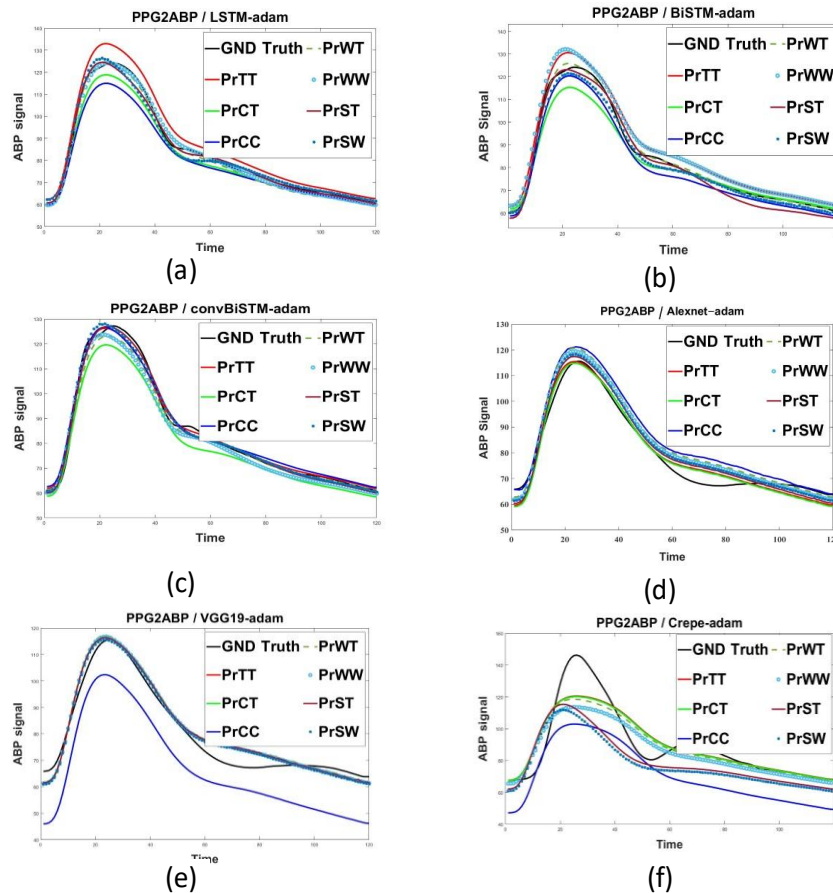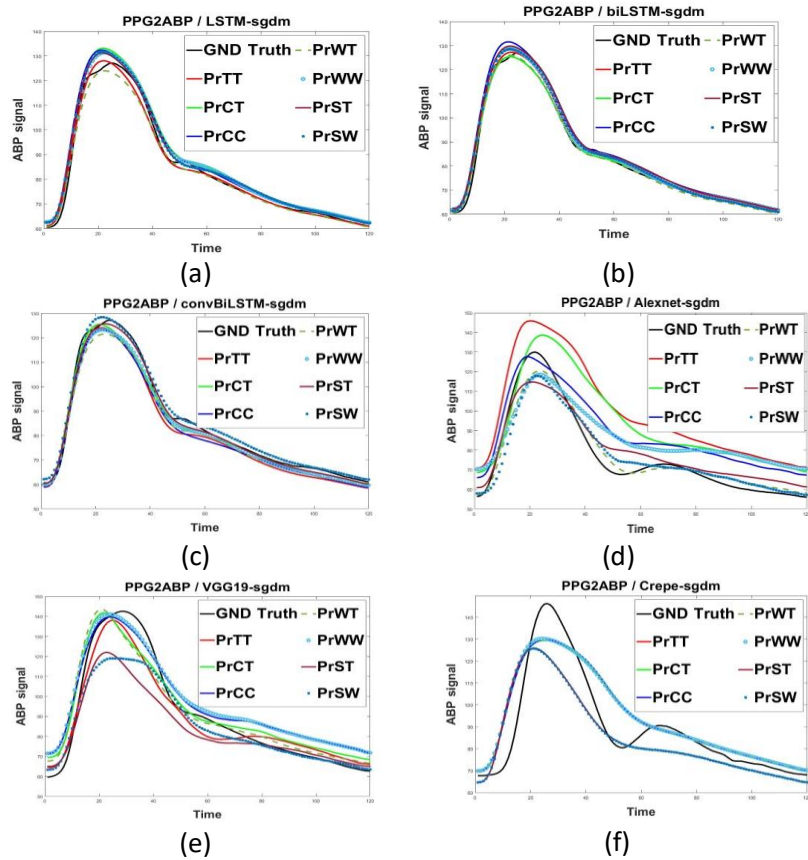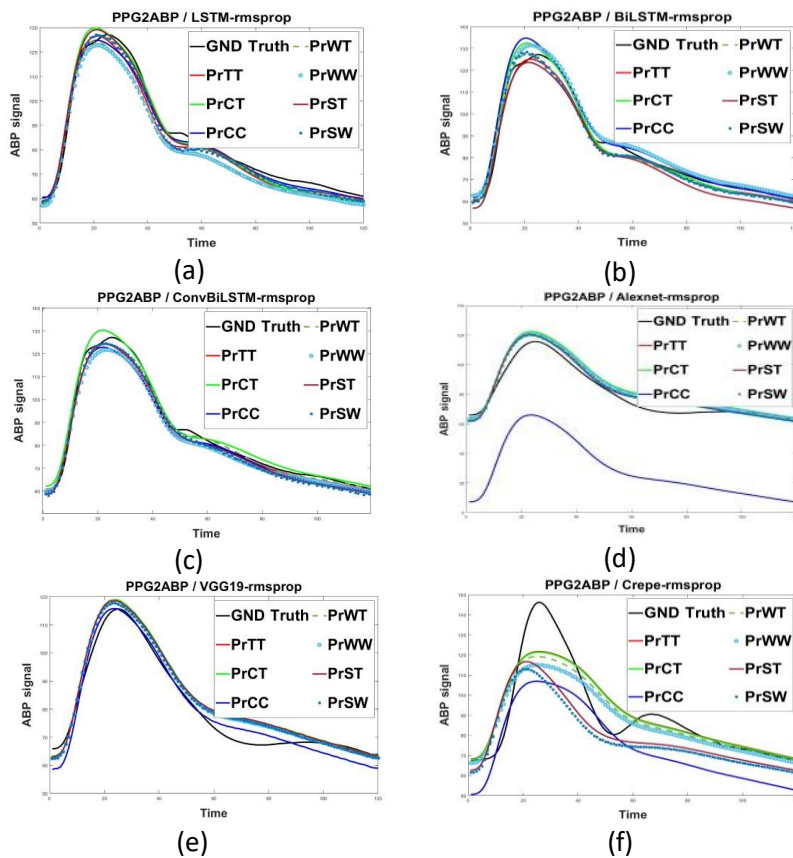

Figure 5. ABP signal Reconstruction from different DNN and different Transformation combinations at RMSProp optimizer (a) LSTM, (b) BiLSTM, (c) Proposed ConvBiLSTM, (d) Alexnet, (e) VGG19, and (f) crepe

Figure 4 depicts an illustrative instance of the reconstructed ABP beats, utilizing distinct feature domains and various DNNs, in comparison to the authentic ABP beat for the SGDM optimizer. The figure demonstrates a strong correlation between the estimated ABP beat obtained through CT and CC methods and the ground truth ABP beat for the BiLSTM NN, in comparison to various other DNNs. The proposed ConvBiLSTM NN demonstrates a strong correlation between the ST and SW feature domains and the ground truth.

Figure 5 shows an example of the reconstructed ABP beats with different feature domains and different DNNs compared to the ground truth ABP beat for RMSProp optimizer. As shown from this figure, the estimated ABP beat by using SW and ST are highly related and correlated to the ground truth ABP beat for the proposed ConvBiLSTM NN compared with other different DNNs.

4.3 Blood pressure estimation results

Metrics such as mean error (ME) and standard deviation (STD) were used to evaluate our SBP and DBP values. These tables show ADAM optimizer's SBP and DBP prediction performance data. The model predicted DBP better than SBP. However, the measurement factor values are fairly well, indicating that the proposed model can accurately and easily measure SBP and DBP.

Tables 5 and 6 present a comparative analysis of various feature domains in terms of standard deviation (STD) and mean absolute error (MAE) for the estimated systolic blood pressure (SBP) and diastolic blood pressure (DBP). Based on the presented tables, it is evident that the choice of utilizing the time domain, discrete cosine transform (DCT) domain, or discrete wavelet transform (DWT) domain has a negligible impact on blood pressure (BP) estimation. This can be attributed to the susceptibility of these domains to variations in beat shift and scale. However, the utilization of SWT has been acknowledged to enhance the STD and MAE as a result of improved feature localization and reduced sensitivity to shifting and scaling. Table 5 displays the performance results for SBP, indicating that the Proposed convBiLSTM NN exhibits the most accurate estimation at the SW feature domain. The STD and MAE of the SBP for the proposed NN are 15.65 mmHg and 12.01 mmHg, respectively. Additionally, Table 6 presents the performance results for DBP, indicating that the Proposed convBiLSTM NN achieves the most accurate estimation at SW. The STD and MAE of the DBP for the proposed NN are 7.07 mmHg and 5.44 mmHg, respectively.

Table 2. PPG2ABP RMSE comparison for ADAM optimizer

Network	SW	ST	WW	WT	CC	CT	TT
LSTM	6.53	6.37	8.16	8.07	6.2	6.24	8.37
BiLSTM	6.62	6.38	8.06	8.09	**6.13**	<u>**6.11**</u>	8.38
Proposed (ConvBiLSTM)	**6.51**	**6.23**	8.39	8.33	6.41	6.29	8.29
Alexnet	8.21	7.74	7.60	7.34	7.05	8.04	9.17
VGG19	7.54	7.54	8.45	7.84	8.29	7.88	7.62
Crepe	7.01	7.02	**6.84**	**6.83**	6.82	6.81	**6.82**

Table 3. PPG2ABP RMSE comparison for SGDM optimizer

Network	SW	ST	WW	WT	CC	CT	TT
LSTM	7.06	7.88	8.73	8.76	6.75	6.71	9.21
Bi-LSTM	7.44	7.07	8.78	8.69	6.80	6.71	9.17
Proposed (ConvBiLSTM)	<u>**6.53**</u>	**6.67**	7.31	8.73	**6.54**	**6.56**	8.79
Alexnet	6.76	6.79	**6.62**	**6.59**	6.78	6.80	**6.69**
VGG-19	7.03	7.22	7.13	7.10	7.33	7.09	7.72
Crepe	7.14	6.90	6.88	6.75	15.05	6.73	6.74

Table 4. PPG2ABP RMSE comparison for RMSProp optimizer

Network	SW	ST	WW	WT	CC	CT	TT
LSTM	6.89	6.97	8.48	8.54	6.51	6.45	8.86
BiLSTM	6.85	6.87	8.51	8.46	6.48	6.38	8.97
Proposed (ConvBiLSTM)	<u>**6.35**</u>	**6.72**	8.78	8.98	**6.37**	**6.44**	8.93
Alexnet	7.27	7.21	7.2	7.17	12.20	7.27	7.26
VGG19	7.27	7.3	7.43	7.33	7.98	7.32	7.32
Crepe	7.17	6.98	**6.96**	**6.87**	11.10	6.85	**6.84**

Table 5. SBP STD and MAE performance comparison

Network	SW		ST		WW		WT		CC		CT		TT	
	STD	MAE	STD	MAE	STD	MAE	STD	MAE	STD	MAE	STD	MAE	STD	MAE
LSTM [35]	17.1	13.3	17.8	14.0	18.6	14.4	18.7	14.5	16.2	12.4	16.1	12.3	19.3	15.0
BiLSTM [37]	17.4	13.7	17.1	13.4	18.6	14.4	18.5	14.3	16.0	12.2	16.1	12.2	19.2	14.9
Proposed (convBiLSTM)	<u>**15.6**</u>	<u>**12.0**</u>	**16.2**	**12.5**	18.6	**14.4**	18.8	**14.5**	**15.7**	**12.1**	**15.9**	**12.1**	18.8	14.5
Alexnet [43]	17.7	20.9	17.7	14.5	**17.6**	20.8	**17.6**	14.4	23.8	25.2	17.6	14.3	**17.6**	**14.4**
VGG19 [45]	17.8	23.1	17.7	16.2	17.9	23.9	17.8	16.7	19.7	27.5	17.8	16.8	17.8	16.8
Crepe	17.9	20.1	17.8	15.7	18.3	22.5	18.0	15.2	24.3	24.6	17.9	15.1	18.0	15.2

Table 6. DBP STD and MAE performance comparison

Network	SW		ST		WW		WT		CC		CT		TT	
	STD	MAE	STD	MAE	STD	MAE	STD	MAE	STD	MAE	STD	MAE	STD	MAE
LSTM [35]	7.75	5.87	8.4	6.6	9.5	7.32	9.53	7.33	7.74	5.87	7.67	5.83	9.88	7.65
BiLSTM [37]	7.95	6.18	7.65	5.85	9.6	7.38	9.51	7.28	7.69	6.01	7.64	5.85	9.8	7.61
Proposed (convBiLSTM)	<u>**7.07**</u>	<u>**5.44**</u>	**7.11**	**5.46**	9.44	**7.22**	9.48	**7.25**	**7.69**	**5.64**	**7.77**	**5.83**	9.49	7.29
Alexnet [43]	8.90	12.24	8.76	6.73	**8.91**	20.82	**8.67**	6.69	9.78	13.01	8.78	6.93	**8.78**	**6.92**
VGG19 [45]	8.93	16.10	8.94	6.90	8.94	16.53	8.94	6.94	8.90	20.42	8.98	6.98	8.98	6.98
Crepe	8.94	23.19	8.98	6.94	8.94	24.09	9.11	7.02	9.98	19.94	9.11	7.04	9.13	7.05

5. CONCLUSIONS

In the present study, we aimed to infer the full heartbeat of BP signals from PPG alone. There are actually a number of businesses that calculate important information such as DBP and SBP. However, none of these studies were able to provide a comprehensive picture of BP., that is, the full waveform. In addition, they frequently required additional signals, such as an ECG, to aid in the calculation. Furthermore, many algorithms compute some handcrafted features of the signals as an essential pre-processing step, needs properly structured signals without any noise or artefacts to work. Thus, in addition to demonstrating better performance in DBP and SBP predictions even though we were not explicitly trained to do so, our work develops state of the art in three different dimensions, First, we compare between the proposed convBiLSTM NN system for PPG-ABP estimation and BP estimation with different NNs which are two 1D DNN (LSTM and BiLSTM), with 1D audio network (crepe), and with two 2D image DNN (Alexnet and VGG19)

Second, we compare between the proposed scattering transformation for convBiLSTM NN system for PPG-ABP estimation and BP estimation with different combinations of transformation (TT, CT, CC, WT, WW, ST, and SW). Third, we compare between different optimizers (ADAM, SGDM, and RMSProp) for different NNs and different Transformation combinations.

REFERENCES

[1] World Health Organization. https://www.who.int/news-room/fact-sheets/detail.

[2] Lim, P.K., Ng, S.C., Jassim, W.A., Redmond, S.J., Zilany, M., Avolio, A., Lim, E., Tan, M.P., Lovell, N.H. (2015). Improved measurement of blood pressure by extraction of characteristic features from the cuff oscillometric waveform. Sensors, 15(6): 14142-14161. https://doi.org/10.3390/s150614142

[3] Miao, F., Liu, Z.D., Liu, J.K., Wen, B., He, Q.Y., Li, Y. (2019). Multi-sensor fusion approach for cuff-less blood pressure measurement. IEEE Journal of Biomedical and Health Informatics, 24(1): 79-91. https://doi.org/10.1109/JBHI.2019.2901724

[4] Martínez, G., Howard, N., Abbott, D., Lim, K., Ward, R., Elgendi, M. (2018). Can photoplethysmography replace arterial blood pressure in the assessment of blood pressure? Journal of Clinical Medicine, 7(10): 316. https://doi.org/10.3390/jcm7100316

[5] Mukkamala, R., Hahn, J.O., Inan, O.T., Mestha, L.K., Kim, C.S., Töreyin, H., Kyal, S. (2015). Toward ubiquitous blood pressure monitoring via pulse transit time: theory and practice. IEEE Transactions on Biomedical Engineering, 62(8): 1879-1901. https://doi.org/10.1109/TBME.2015.2441951

[6] Esmaili, A., Kachuee, M., Shabany, M. (2017). Nonlinear cuffless blood pressure estimation of healthy subjects using pulse transit time and arrival time. IEEE Transactions on Instrumentation and Measurement, 66(12): 3299-3308. https://doi.org/10.1109/TIM.2017.2745081

[7] Kachuee, M., Kiani, M.M., Mohammadzade, H., Shabany, M. (2016). Cuffless blood pressure estimation algorithms for continuous health-care monitoring. IEEE Transactions on Biomedical Engineering, 64(4): 859-869. https://doi.org/10.1109/TBME.2016.2580904

[8] Wagenseil, J.E., Mecham, R.P. (2012). Elastin in large artery stiffness and hypertension. Journal of Cardiovascular Translational Research, 5: 264-273. https://doi.org/10.1007/s12265-012-9349-8

[9] Liu, M., Po, L.M., Fu, H. (2017). Cuffless blood pressure estimation based on photoplethysmography signal and its second derivative. International Journal of Computer Theory and Engineering, 9(3): 202.

[10] Teng, X.F., Zhang, Y.T. (2003). Continuous and noninvasive estimation of arterial blood pressure using a photoplethysmographic approach. In Proceedings of the 25th Annual International Conference of the IEEE Engineering in Medicine and Biology Society (IEEE Cat. No. 03CH37439), 4: 3153-3156. https://doi.org/10.1109/IEMBS.2003.1280811

[11] Tanveer, M.S., Hasan, M.K. (2019). Cuffless blood pressure estimation from electrocardiogram and photoplethysmogram using waveform based ANN-LSTM network. Biomedical Signal Processing and Control, 51: 382-392. https://doi.org/10.1016/j.bspc.2019.02.028

[12] Suzuki, A., Ryu, K. (2013). Feature selection method for estimating systolic blood pressure using the Taguchi method. IEEE Transactions on Industrial Informatics, 10(2): 1077-1085. https://doi.org/10.1109/TII.2013.2288498

[13] Fujita, D., Suzuki, A., Ryu, K. (2019). PPG-based systolic blood pressure estimation method using PLS and level-crossing feature. Applied Sciences, 9(2): 304. https://doi.org/10.3390/app9020304

[14] Khalid, S.G., Zhang, J., Chen, F., Zheng, D. (2018). Blood pressure estimation using photoplethysmography only: comparison between different machine learning approaches. Journal of Healthcare Engineering, 2018: 1548647. https://doi.org/10.1155/2018/1548647

[15] Zhang, B., Wei, Z., Ren, J., Cheng, Y., Zheng, Z. (2018). An empirical study on predicting blood pressure using classification and regression trees. IEEE Access, 6: 21758-21768. https://doi.org/10.1109/ACCESS.2017.2787980

[16] Chen, Y., Cheng, J., Ji, W.Q. (2019). Continuous blood pressure measurement based on photoplethysmography. In 2019 14th IEEE International Conference on Electronic Measurement & Instruments (ICEMI), Changsha, China, pp. 1656-1663. https://doi.org/10.1109/ICEMI46757.2019.9101774

[17] Mousavi, S.S., Firouzmand, M., Charmi, M., Hemmati, M., Moghadam, M., Ghorbani, Y. (2019). Blood pressure estimation from appropriate and inappropriate PPG signals using A whole-based method. Biomedical Signal Processing and Control, 47: 196-206. https://doi.org/10.1016/j.bspc.2018.08.022

[18] Miao, F., Fu, N., Zhang, Y.T., Ding, X.R., Hong, X., He, Q., Li, Y. (2017). A novel continuous blood pressure estimation approach based on data mining techniques. IEEE Journal of Biomedical and Health Informatics, 21(6): 1730-1740. https://doi.org/10.1109/JBHI.2017.2691715

[19] Chen, S., Ji, Z., Wu, H., Xu, Y. (2019). A non-invasive continuous blood pressure estimation approach based on machine learning. Sensors, 19(11): 2585. https://doi.org/10.3390/s19112585

[20] Park, J.U., Kang, D.W., Erdenebayar, U., Kim, Y.J., Cha, K.C., Lee, K.J. (2020). Estimation of arterial blood pressure based on artificial intelligence using single earlobe photoplethysmography during cardiopulmonary resuscitation. Journal of Medical Systems, 44: 1-4. https://doi.org/10.1007/s10916-019-1514-z

[21] Senturk, U., Polat, K., Yucedag, I. (2020). A non-invasive continuous cuffless blood pressure estimation using dynamic recurrent neural networks. Applied Acoustics, 170: 107534. https://doi.org/10.1016/j.apacoust.2020.107534

[22] Esmaelpoor, J., Moradi, M.H., Kadkhodamohammadi, A. (2020). A multistage deep neural network model for blood pressure estimation using photoplethysmogram signals. Computers in Biology and Medicine, 120: 103719. https://doi.org/10.1016/j.compbiomed.2020.103719

[23] Baek, S., Jang, J., Yoon, S. (2019). End-to-end blood pressure prediction via fully convolutional networks. IEEE Access, 7: 185458-185468. https://doi.org/10.1109/ACCESS.2019.2960844

[24] Slapničar, G., Mlakar, N., Luštrek, M. (2019). Blood pressure estimation from photoplethysmogram using a spectro-temporal deep neural network. Sensors, 19(15): 3420. https://doi.org/10.3390/s19153420

[25] Landry, C., Peterson, S.D., Arami, A. (2020). Nonlinear dynamic modeling of blood pressure waveform: Towards an accurate cuffless monitoring system. IEEE Sensors Journal, 20(10): 5368-5378. https://doi.org/10.1109/JSEN.2020.2967759

[26] Ibtehaz, N., Mahmud, S., Chowdhury, M.E., Khandakar, A., Ayari, M.A., Tahir, A., Rahman, M.S. (2020). Ppg2abp: Translating photoplethysmogram (ppg) signals to arterial blood pressure (ABP) waveforms using fully convolutional neural networks. arXiv preprint arXiv:2005.01669. https://arxiv.org/abs/2005.01669

[27] Athaya, T., Choi, S. (2021). An estimation method of continuous non-invasive arterial blood pressure waveform using photoplethysmography: A U-Net architecture-based approach. Sensors, 21(5): 1867. https://doi.org/10.3390/s21051867

[28] Goldberger, A.L., Amaral, L.A., Glass, L., Hausdorff, J.M., Ivanov, P.C., Mark, R.G., Mietus, J.E., Moody, G.B., Peng, C.K., Stanley, H.E. (2000). PhysioBank, PhysioToolkit, and PhysioNet: Components of a new research resource for complex physiologic signals. Circulation, 101(23): e215-e220. https://doi.org/10.1161/01.CIR.101.23.e215

[29] Kachuee, M., Kiani, M.M., Mohammadzade, H., Shabany, M. (2015). Cuff-less high-accuracy calibration-free blood pressure estimation using pulse transit time. In 2015 IEEE International Symposium on Circuits and Systems (ISCAS), pp. 1006-1009. https://doi.org/10.1109/ISCAS.2015.7168806

[30] Salah, M., Omer, O.A., Hassan, L., Ragab, M., Hassan, A.M., Abdelreheem, A. (2022). Beat-based PPG-ABP cleaning technique for blood pressure estimation. IEEE Access, 10: 55616-55626. https://doi.org/10.1109/ACCESS.2022.3175436

[31] Roy, A.B., Dey, D., Mohanty, B., Banerjee, D. (2012). Comparison of FFT, DCT, DWT, WHT compression techniques on electrocardiogram and photoplethysmography signals. In IJCA Special Issue on International Conference on Computing, Communication and Sensor Network CCSN, pp. 6-11.

[32] Asadi, F., Mollakazemi, M.J., Uzelac, I., Moosavian, S.A.A. (2015). A novel method for arterial blood pressure pulse detection based on a new coupling strategy and discrete wavelet transform. In 2015 Computing in Cardiology Conference (CinC), pp. 1081-1084. https://doi.org/10.1109/CIC.2015.7411102

[33] Bruna, J., Mallat, S. (2013). Invariant scattering convolution networks. IEEE Transactions on Pattern Analysis and Machine Intelligence, 35(8): 1872-1886. https://doi.org/10.1109/TPAMI.2012.230

[34] Jean Effil, N., Rajeswari, R. (2022). Wavelet scattering transform and long short-term memory network-based noninvasive blood pressure estimation from photoplethysmograph signals. Signal, Image and Video Processing, 16(1): 1-9. https://doi.org/10.1007/s11760-021-01952-z

[35] Harfiya, L.N., Chang, C.C., Li, Y.H. (2021). Continuous blood pressure estimation using exclusively photopletysmography by LSTM-based signal-to-signal translation. Sensors, 21(9): 2952. https://doi.org/10.3390/s21092952

[36] Gers, F.A., Schraudolph, N.N., Schmidhuber, J. (2002). Learning precise timing with LSTM recurrent networks. Journal of Machine Learning Research, 3(Aug): 115-143.

[37] Lee, D., Kwon, H., Son, D., Eom, H., Park, C., Lim, Y., Seo, C., Park, K. (2020). Beat-to-beat continuous blood pressure estimation using bidirectional long short-term memory network. Sensors, 21(1): 96. https://doi.org/10.3390/s21010096

[38] Kiperwasser, E., Goldberg, Y. (2016). Simple and accurate dependency parsing using bidirectional LSTM feature representations. Transactions of the Association for Computational Linguistics, 4: 313-327. https://doi.org/10.1162/tacl_a_00101

[39] Schuster, M., Paliwal, K.K. (1997). Bidirectional recurrent neural networks. IEEE transactions on Signal Processing, 45(11): 2673-2681. https://doi.org/10.1109/78.650093

[40] Li, Y.H., Harfiya, L.N., Chang, C.C. (2021). Featureless blood pressure estimation based on photoplethysmography signal using CNN and BiLSTM

for IoT devices. Wireless Communications and Mobile Computing, 2021: 1-10. https://doi.org/10.1155/2021/9085100

[41] Xiao, H., Liu, C., Zhang, B. (2022). Reconstruction of central arterial pressure waveform based on CNN-BILSTM. Biomedical Signal Processing and Control, 74: 103513. https://doi.org/10.1016/j.bspc.2022.103513

[42] Kim, J.W., Salamon, J., Li, P., Bello, J.P. (2018). Crepe: A convolutional representation for pitch estimation. In 2018 IEEE International Conference on Acoustics, Speech and Signal Processing (ICASSP), Calgary, AB, Canada, pp. 161-165. https://doi.org/10.1109/ICASSP.2018.8461329

[43] Slapničar, G., Mlakar, N., Luštrek, M. (2019). Blood pressure estimation from photoplethysmogram using a spectro-temporal deep neural network. Sensors, 19(15): 3420. https://doi.org/10.3390/s19153420

[44] Wang, W., Mohseni, P., Kilgore, K.L., Najafizadeh, L. (2021). Cuff-less blood pressure estimation from photoplethysmography via visibility graph and transfer learning. IEEE Journal of Biomedical and Health Informatics, 26(5): 2075-2085. https://doi.org/10.1109/JBHI.2021.3128383

[45] Pu, Y., Xie, X., Xiong, L., Zhang, H. (2021). Cuff-less blood pressure estimation from electrocardiogram and photoplethysmography based on VGG19-LSTM network. Computer Methods in Medicine and Health Care.

[46] Lawrence, S., Giles, C.L., Tsoi, A.C., Back, A.D. (1997). Face recognition: A convolutional neural-network approach. IEEE Transactions on Neural Networks, 8(1): 98-113. https://doi.org/10.1109/72.554195

[47] Ronneberger, O., Fischer, P., Brox, T. (2015). U-net: Convolutional networks for biomedical image segmentation. In Medical Image Computing and Computer-Assisted Intervention–MICCAI 2015: 18th International Conference, Munich, Germany, October 5-9, 2015, Proceedings, Part III 18, pp. 234-241. https://doi.org/10.1007/978-3-319-24574-4_28

NOMENCLATURE

ABP	Arterial blood pressure
CNN	Convolutional neural network
DCT	Discrete cosine transform
DNN	Deep neural network
DWT	Discrete wavelet transform
ECG	Electrocardiogram
GAN	Generative adversarial network
BiLSTM	Bidirectional Long short-term memory
PGAN	Personalized GAN
PPG	Photoplethysmography
SWT	Scattering wavelet transform
TD	Time domain

Greek symbols

$\emptyset$	The Scalling Function
λ	The scale of the filter bank
ψ	The wavelet cluster (Mother Wavelet)

Subscripts

S_x	The invariant part
U_x	The covariant portion